



**Repositorio Institucional de la Universidad Autónoma de Madrid**

<https://repositorio.uam.es>

Esta es la **versión de autor** del artículo publicado en:

This is an **author produced version** of a paper published in:

CrystEngComm 21.9 (2019):1423-1432

**DOI:** <http://dx.doi.org/10.1039/C8CE01916A>

**Copyright:** © The Royal Society of Chemistry 2019

El acceso a la versión del editor puede requerir la suscripción del recurso

Access to the published version may require subscription

# Synthesis and Structural Characterization of Transition Metal Dithiolene Derivatives Containing Divalent Metals as Counter-Cations

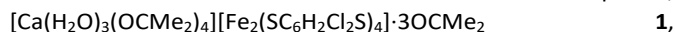
Oscar Castillo,<sup>a</sup> Esther Delgado,<sup>\*,b</sup> Diego Hernández,<sup>b</sup> Elisa Hernández,<sup>b</sup> Avelino Martín,<sup>c</sup> and Félix Zamora<sup>\*,b,d</sup>

Direct reactions between  $\text{HSC}_6\text{H}_4\text{Cl}_2\text{SH}$ ,  $\text{FeCl}_3 \cdot 6\text{H}_2\text{O}$  and divalent metal bases lead to the formation of the cation-anion metal-dithiolene complexes  $[\text{Ca}(\text{H}_2\text{O})_3(\text{OCMe}_2)_4][\text{Fe}_2(\text{SC}_6\text{H}_4\text{Cl}_2\text{S})_4] \cdot 3\text{OCMe}_2$  and  $[\text{Zn}(\text{DMF})_6][\text{Fe}_2(\text{SC}_6\text{H}_4\text{Cl}_2\text{S})_4]$ , as well as the molecular compound  $[\text{Ba}(\text{OCMe}_2)_6][\text{Fe}_2(\text{SC}_6\text{H}_4\text{Cl}_2\text{S})_4]$ , instead of metal-dithiolene coordination polymers as compared with results previously obtained when alkali metals, under similar conditions, were used. An alternative synthetic route based on the reactions between  $\text{K}_2[\text{Fe}_2(\text{SC}_6\text{H}_4\text{Cl}_2\text{S})_4]$  and  $\text{ZnCl}_2 \cdot 6\text{H}_2\text{O}$  or  $\text{NiCl}_2 \cdot 6\text{H}_2\text{O}$  was also evaluated, giving rise to the ion-pair compounds  $[\text{Fe}(\text{H}_2\text{O})_2(\text{THF})_4][\text{Ni}(\text{SC}_6\text{H}_4\text{Cl}_2\text{S})_2]_2 \cdot 4\text{THF}$  and  $[\text{Fe}(\text{H}_2\text{O})_4(\text{THF})_2][\text{Fe}_2(\text{SC}_6\text{H}_4\text{Cl}_2\text{S})_4] \cdot 4\text{THF}$  and the coordination polymer  $\{[\text{K}_2(\text{THF})_8][\text{Zn}_6(\mu\text{-Cl})_2(\text{SC}_6\text{H}_4\text{Cl}_2\text{S})_4(\mu\text{-K}:\text{O}:\text{K}:\text{O}':\text{SC}_6\text{H}_4\text{Cl}(\text{ClO}_2\text{S})_2)]_n\}$ . It is interesting to remark that in the last compound the oxidation of one Cl substituent of a dithiolene ligand yielded the formation of a  $\text{Cl}(\text{O})_2$  group.

## Introduction

For a long time, coordination chemistry of transition metals bearing dithiolene ligands is a research field of high interest because of the potential interesting electronic properties, such as magnetism and/or electrical conductivity, that these compounds can show, as well as the wide structural diversity showed by them.<sup>1-15</sup> However, most of the studies have been focused on mononuclear compounds. Recently, we have reported a series of coordination polymers containing the dianionic entities  $[\text{Fe}_2(\text{SC}_6\text{H}_4\text{R}_2\text{S})_4]^{2-}$  ( $\text{R} = \text{Cl}, \text{H}$ ) and  $[\text{M}_2(\mu\text{-L})_n]^{2+}$  ( $\text{M} = \text{alkali metal}$ ) as counter-cations.<sup>16, 17</sup>

Taking into account these results we have considered of interest to study the possibility to form coordination polymers (CPs) containing cationic divalent metals instead, in order to evaluate their structural effects on the coordination metal-dithiolene network rearrangement. Here we report on the reactions carried out between  $\text{HSC}_6\text{H}_4\text{Cl}_2\text{SH}$ ,  $\text{FeCl}_3 \cdot 6\text{H}_2\text{O}$  and divalent metal bases which lead to the formation of cation-anion metal complexes,



<sup>a</sup> Departamento de Química Inorgánica, Universidad del País Vasco (UPV/EHU), Apartado 644, 48080 Bilbao, Spain.

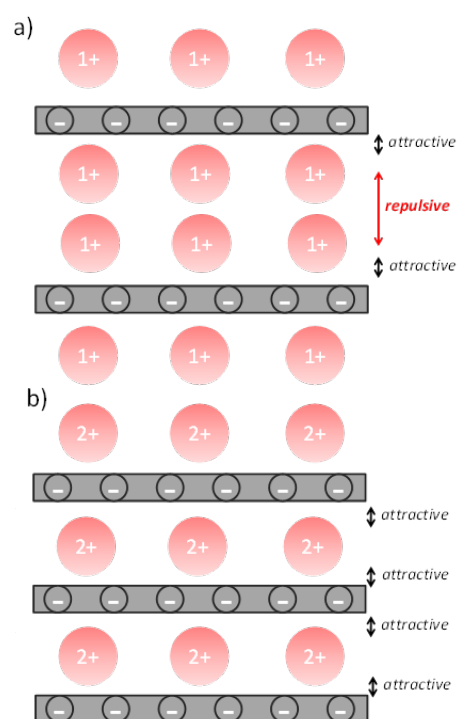
<sup>b</sup> Departamento de Química Inorgánica, Universidad Autónoma de Madrid, 28049 Madrid, Spain.

<sup>c</sup> Departamento de Química Orgánica y Química Inorgánica, Universidad de Alcalá. Campus Universitario, E-28805, Alcalá de Henares, Spain.

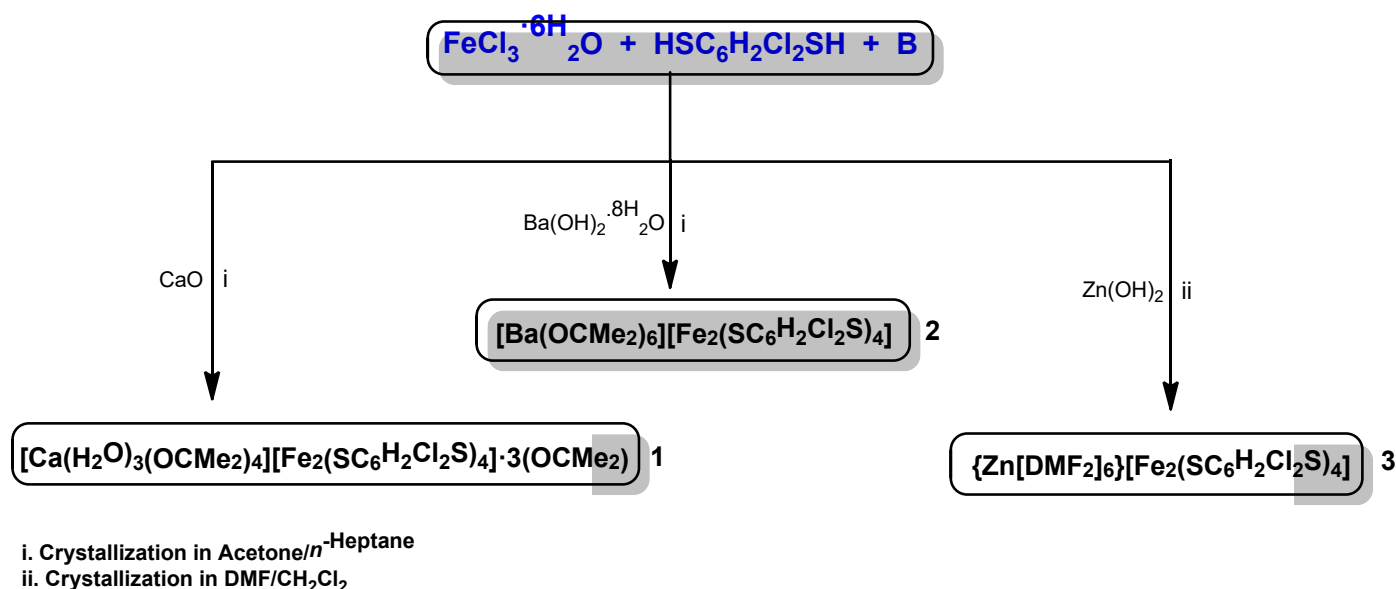
<sup>d</sup> Instituto Madrileño de Estudios Avanzados en Nanociencia (IMDEA Nanociencia), Cantoblanco, 28049 Madrid, Spain.

† Electronic Supplementary Information (ESI) available: additional structural information is available free of charge. Files in CIF format for compounds **1-7** are [CCDC 1834784 (**1**), 1834781 (**2**), 1834783 (**3**), 1834785 (**4**), 1834789 (**5**), 1834786 (**6**), 1834788 (**7**)] available free of charge. See DOI: 10.1039/x0xx00000x

$[\text{Ba}(\text{OCMe}_2)_6][\text{Fe}_2(\text{SC}_6\text{H}_4\text{Cl}_2\text{S})_4] \quad \mathbf{2},$  and  $\{\text{Zn}(\text{DMF})_6[\text{Fe}_2(\text{SC}_6\text{H}_4\text{Cl}_2\text{S})_4]\} \quad \mathbf{3},$  instead of the CPs formed in the analogous reactions using alkali metals instead.<sup>16, 17</sup>



**Scheme 1.** Electrostatic interactions taking place between an anionic 1D polymeric chain and monovalent (a) versus divalent cationic entities to counterbalance the charge (b).



**Scheme 2.** Summary of reactions to obtain compounds 1-3.

Additionally, the reactions carried out between  $\text{K}_2[\text{Fe}_2(\text{SC}_6\text{H}_2\text{Cl}_2\text{S})_4]$  and  $\text{ZnCl}_2 \cdot 6\text{H}_2\text{O}$  or  $\text{NiCl}_2 \cdot 6\text{H}_2\text{O}$  give rise to the new compounds  $[\text{Fe}(\text{H}_2\text{O})_4(\text{THF})_2][\text{Fe}_2(\text{SC}_6\text{H}_2\text{Cl}_2\text{S})_4] \cdot 4\text{THF}$  **4**,  $\{[\text{K}_2(\text{THF})_8][\text{Zn}_6(\mu\text{-Cl})_2(\text{SC}_6\text{H}_2\text{Cl}_2\text{S})_4(\mu\text{-}\kappa\text{O}':\kappa\text{O}'\text{-SC}_6\text{H}_2\text{Cl}(\text{ClO}_2)\text{S})_2]\}_n$  **5** and  $[\text{Fe}(\text{H}_2\text{O})_2(\text{THF})_4][\text{Ni}(\text{SC}_6\text{H}_2\text{Cl}_2\text{S})_2]_2 \cdot 4\text{THF}$  **6**.

## Results and discussion

We have previously observed the formation of 1D CPs with different architectures based on the assemble of dianionic entities  $[\text{Fe}_2(\text{SC}_6\text{H}_2\text{R}_2\text{S})_4]^{2-}$  ( $\text{R} = \text{Cl}, \text{H}$ ) and cationic moieties  $[\text{M}_2(\mu\text{-L})_n]^{2+}$  ( $\text{M} = \text{group 1 metal}$ ) depending upon the size of the alkali metal, as well as the crystallization conditions (*i.e.* different organic solvents, presence/absence of water).<sup>16, 17</sup> In all of these CPs the positive charge density of the alkali complexes must match that of the  $[\text{Fe}_2(\text{SC}_6\text{H}_2\text{R}_2\text{S})_4]^{2-}$  ( $\text{R} = \text{Cl}, \text{H}$ ) anionic complexes and electron repulsive forces are present in the two monovalent cations of the entity  $[\text{M}_2(\mu\text{-L})_n]^{2+}$  (Scheme 1a).

We have now tried to evaluate whether the use of divalent cation complexes as counter cations instead, could favor the formation of different coordination polymers, as they do not show these electron repulsive forces (Scheme 1b).

Initially, we carried out the reaction between  $\text{FeCl}_3 \cdot 6\text{H}_2\text{O}$  with the dithiolene  $\text{HSC}_6\text{H}_2\text{Cl}_2\text{SH}$  in the presence of  $\text{CaO}$  as deprotonating agent (Scheme 2). Diffraction studies carried out on crystals obtained in this reaction confirmed the formation of compound **1**. The structure of **1** consists of an ion-pair molecule formed by the dianionic entity  $[\text{Fe}_2(\text{SC}_6\text{H}_2\text{Cl}_2\text{S})_4]^{2-}$  and a cationic  $\text{Ca}(\text{II})$  complex.

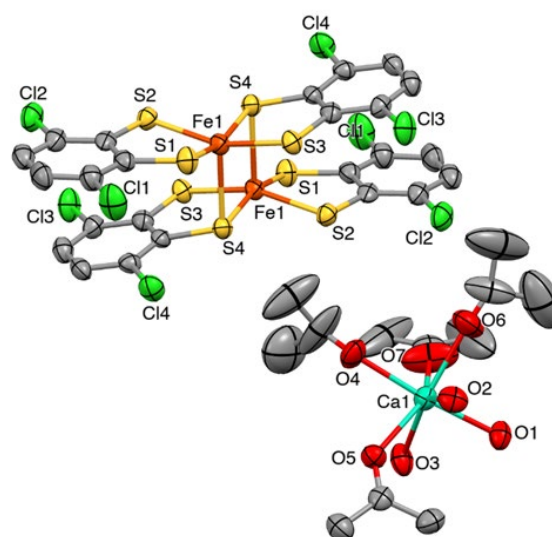


**Fig. 1.** ORTEP diagram of the molecular unit of compound **1**. Hydrogen atoms have been omitted for clarity. Thermal ellipsoids are drawn at 50 % probability.

The structure of compound **1** shows two independent  $\text{Fe}(\text{SC}_6\text{H}_2\text{Cl}_2\text{S})_2$  moieties, which are related with the other half of the dianionic unit by a center of symmetry. Fig. 1 shows the cationic fragment together with the  $\text{Fe}(1)$  independent iron dianionic moiety.

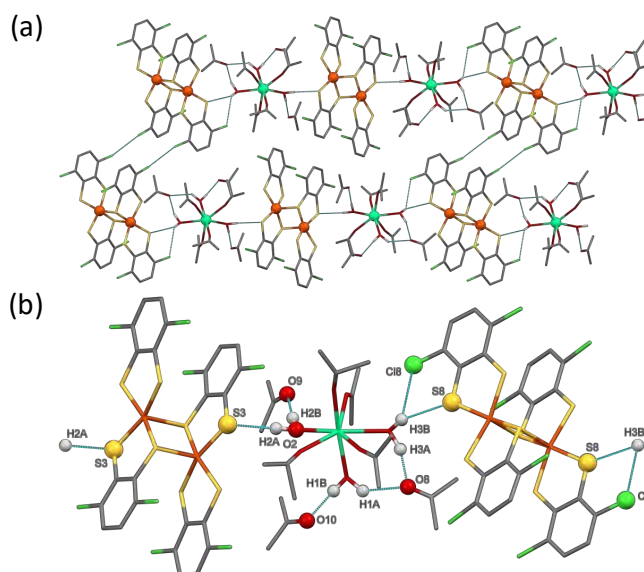
**Table 1.** Ranges for selected bond distances (Å) found for compounds 1-7.

Compound	C=C	C-S	M-S	M'-S	M'-O
1	1.406(9)- 1.426(9)	1.761(6)- 1.777(6)	2.223(2)- 2.510(2)		2.356(5)- 2.452(5)
2	1.411(1)- 1.437(1)	1.744(1)- 1.770(1)	2.221(3)- 2.508(3)	3.511(3)- 3.359(3)	2.603(8)- 2.797(9)
3	1.396(6) 1.400(6)	1.750(4)- 1.758(4)	2.211(1)- 2.497(1)		2.028(3)- 2.126(3)
4	1.392(9)- 1.412(1)	1.749(7)- 1.761(6)	2.216(2)- 2.493(2)		2.192(5)- 2.208(4)
5	1.392(9)- 1.41(1)	1.710(7)- 1.784(6)	2.322(2)- 2.375(2)		2.682(7)- 2.856(5)
6	1.403(4)- 1.404(5)	1.732(3)- 1.738(3)	2.143(1)- 2.148(1)		2.026(3)- 2.215(2)
7	1.388(4)- 1.394(3)	1.756(2)- 1.769(2)	2.225(1)- 2.456(1)	3.251(1)- 3.661(1)	2.728(2)- 2.746(2)

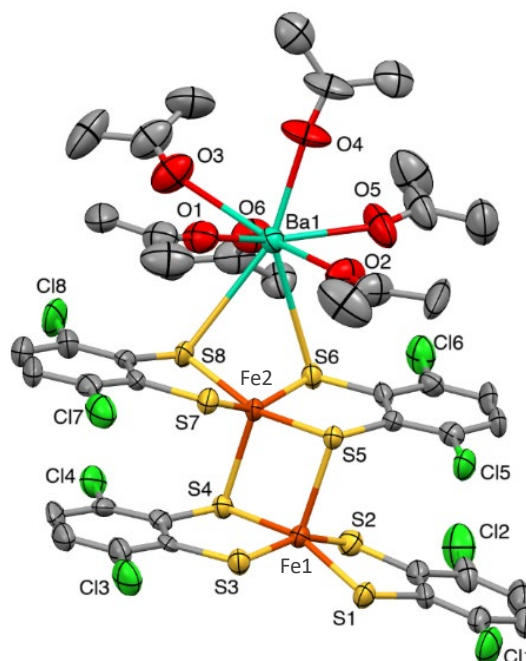
The dianionic unit  $[\text{Fe}_2(\text{SC}_6\text{H}_2\text{Cl}_2\text{S})_4]^{2-}$  displays the same geometry as that previously found in related compounds where each iron atom shows the expected 4 + 1 square-pyramidal geometry.<sup>16, 17</sup> The Fe-S, S-C and C-C distances (Table 1) are also in the range reported for analogous derivatives.<sup>16-23</sup> On the other hand, the Ca(II) atom is heptacoordinated by four acetone and three  $\text{H}_2\text{O}$  molecules yielding to a distorted pentagonal bipyramidal geometry, with an O(1)-Ca(1)-O(4) angle of  $169.4(2)^\circ$  between the apical positions, and a range of  $72.3(2)^\circ$ - $76.1(2)^\circ$  for the angles between the equatorial ligands. The Ca-O distances (Table 1) agree with those reported for similar Ca-O<sub>H2O</sub> bonds<sup>24-32</sup> and Ca-O<sub>acetone</sub>,<sup>32-34</sup> respectively.

Network of **1** shows a weak type-I halogen bonding interaction (Fig. 2a) with Cl(6)⋯Cl(7) of 3.3735(6) Å, 0.13 Å shorter than the sum of the van der Waals radii, with angles C(17)-Cl(6)-Cl(7)  $163.72(1)^\circ$  and C(20)-Cl(7)-Cl(6)  $164.33(1)^\circ$  (Cl(6) and Cl(7) belong to the Fe(2) dianionic unit).<sup>35,36</sup> Additionally, weak O-H⋯O, O-H⋯Cl, and O-H⋯S interactions contribute to build the supramolecular 2D network shown in Fig. 2b (SI for additional data).

To our knowledge, compounds  $[\text{Ca}(12\text{-crown-4})_2][\text{Ni}(\text{dmit})_2]_2$  (dmit = (2-thioxo-1,3-dithiole-4,5-dithiolate),  $[\text{Ca}(15\text{-crown-5})_2][\text{Ni}(\text{dmit})_2]_2(\text{CH}_3\text{CN})_{0.7}$ ,  $[\text{Ca}(18\text{-crown-6})][\text{Ni}(\text{dmit})_2]_2(\text{CH}_3\text{CN})_2$  and  $[\text{Ca}(\text{DA}18\text{-crown-6})][\text{Ni}(\text{dmit})_2]_2(\text{CH}_3\text{CN})_2$  are the only examples reported<sup>37</sup> so far on bis-dithiolene transition metal derivatives containing Ca(II) complexes as counter cations.

**Fig. 2.** a) Partial view along (623) of the supramolecular network generated by compound **1**. b) Detail of the O-H⋯O, O-H⋯Cl, and O-H⋯S interactions. Aromatic hydrogen atoms have been omitted for clarity.

A similar reaction but using  $\text{Ba}(\text{OH})_2 \cdot 8\text{H}_2\text{O}$  as deprotonating agent instead, gave rise the neutral trinuclear compound  $[\text{Ba}(\text{OCMe}_2)_6][\text{Fe}_2(\text{SC}_6\text{H}_2\text{Cl}_2\text{S})_4]$  **2** (Fig. 3). The structure of compound **2** consists of a heterotrimeric coordination compound where  $[\text{Ba}(\text{OCMe}_2)_6]^{2+}$  is connected to the  $[\text{Fe}_2(\text{SC}_6\text{H}_2\text{Cl}_2\text{S})_4]^{2-}$  moiety by coordination to the two sulfur atoms of two dithiolene ligands.

**Fig. 3.** ORTEP diagram of the molecular unit of compound **2**. Hydrogen atoms have been omitted for clarity. Thermal ellipsoids are drawn at 50 % probability.

The barium atom exhibits a bicapped trigonal prism geometry [being O(3) and O(5) the donor atoms of the capping

acetones], with similar Ba-S distances to those found in complexes with the same coordination environment.<sup>38</sup> The Ba-O<sub>acetone</sub> distances [2.603(8)-2.797(9) Å] are in the range found for compounds containing this type of bond.<sup>38-42</sup> As expected, the iron dimer presents similar Fe-S, S-C and C-C distances to those found for compound **1** (Table 1). Finally, no significant interactions have been found in the crystal packing of **2** (Fig. S).

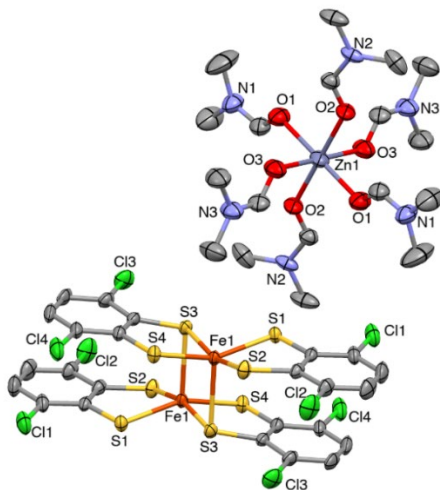


**Fig. 4.** ORTEP diagram of the molecular unit of compound **3**. Hydrogen atoms have been omitted for clarity. Thermal ellipsoids are drawn at 50 % probability.

In order to evaluate the role of another divalent cation such as Zn(II) we tried the direct reaction between  $\text{FeCl}_3 \cdot 6\text{H}_2\text{O}$  with  $\text{HSC}_6\text{H}_4\text{Cl}_2\text{SH}$  and  $\text{Zn}(\text{OH})_2$  as deprotonating agent yielded compound  $[\text{Zn}(\text{DMF})_6][\text{Fe}_2(\text{SC}_6\text{H}_4\text{Cl}_2\text{S})_4]$  **3**.

The crystal structure of **3** (Fig. 4) reveals the formation of an ion-pair compound similar to that found for **1**. As it can be seen in Table 1, geometrical parameters found for the dianionic entity  $[\text{Fe}_2(\text{SC}_6\text{H}_4\text{Cl}_2\text{S})_4]^{2-}$  are similar to those mentioned for compounds **1** and **2** while in the cationic unit  $[\text{Zn}(\text{DMF})_6]^{2+}$ , the Zn(II) is coordinated to six DMF ligands yielding to an octahedral geometry. The crystal packing of **3** (Fig. S23) does not show any significant supramolecular interactions. We have found that compounds  $\{\text{Zn}[\text{Ni}(\text{pedt})_2](\text{DMF})_2\}_n$  (pedt = 1-(pyridine-4-yl)ethylene-1,2-dithiolate).<sup>43</sup>  $[\text{Zn}(\text{C}_2\text{H}_8\text{N}_2)_3][\text{Ni}(\text{C}_4\text{N}_2\text{S}_2)_2]$ <sup>44</sup> and  $[\text{Zn}(\text{C}_2\text{H}_8\text{N}_2)_3][\text{Cu}(\text{C}_4\text{N}_2\text{S}_2)_2]$ <sup>45</sup> are the only compounds of dithiolene derivatives of transition metals where a Zn(II) cation complex neutralize the negative charge. From all of them, only compound  $\{\text{Zn}[\text{Ni}(\text{pedt})_2](\text{DMF})_2\}_n$ <sup>43</sup> is a CP.

In contrast with the behavior previously observed for the alkaline metals which led to CP formation,<sup>17</sup> the reaction under similar conditions using divalent cations (Scheme 2), *i.e.*  $\text{Ca}^{2+}$ ,  $\text{Ba}^{2+}$  or  $\text{Zn}^{2+}$ , failed. This prompted us to try a different strategy to isolated CPs. Thus, we have evaluated the possibility to exchange the two potassium atoms in compound  $\text{K}_2[\text{Fe}_2(\text{SC}_6\text{H}_4\text{Cl}_2\text{S})_4]$  by divalent cations such as  $\text{Zn}^{2+}$  or  $\text{Ni}^{2+}$  (Scheme 3).

Consequently, a mixture of a THF solution of compound  $\text{K}_2[\text{Fe}_2(\text{SC}_6\text{H}_4\text{Cl}_2\text{S})_4]$  and  $\text{ZnCl}_2 \cdot 6\text{H}_2\text{O}$  in EtOH/ $\text{H}_2\text{O}$  was stirred for

1.5 days. The solid residue obtained from this reaction crystallized in THF/*n*-Heptane yielded several crystals of different color and shape corresponding to the starting material  $\text{K}_2[\text{Fe}_2(\text{SC}_6\text{H}_4\text{Cl}_2\text{S})_4]$ , the known salt  $\text{K}_2[\text{ZnCl}_4]$ , and crystals in traces amount of the new compounds  $[\text{Fe}(\text{H}_2\text{O})_4(\text{THF})_2][\text{Fe}_2(\text{SC}_6\text{H}_4\text{Cl}_2\text{S})_4] \cdot 4\text{THF}$  **4** and  $\{\text{K}_2(\text{THF})_8\}[\text{Zn}_6(\mu\text{-Cl})_2(\text{SC}_6\text{H}_4\text{Cl}_2\text{S})_4(\mu\text{-KO}:\text{KO}'\text{-SC}_6\text{H}_4\text{Cl}(\text{ClO}_2)\text{S})_2)]_n$  **5**. Therefore, confirming that a partial transfer reaction of the dithiolene groups accomplished by a ligand oxidation at the dithiolene takes place (Scheme 3).

The presence of only iron atoms in the molecule of **4** was determined by TXRF analysis. As it can be seen in Fig. 5, as a consequence of the substitution of the two potassium atoms in the starting material by an iron atom. In the cationic fragment the iron atom is coordinated to four oxygen atoms of  $\text{H}_2\text{O}$  molecules and two from the THF ligands yielding to a distorted octahedral geometry; bond distances and angles (see range Table 1) are similar to those found for cation in  $[\text{Fe}(\text{H}_2\text{O})_2(\text{THF})_4][\text{Cd}_8\{\text{Fe}(\text{CO})_4\}_4\text{Cl}_9(\text{THF})_6]_2$ .<sup>46</sup>

On the other hand, geometrical parameters found for the dianionic moiety  $[\text{Fe}_2(\text{SC}_6\text{H}_4\text{Cl}_2\text{S})_4]^{2-}$  are very similar to those obtained for complexes **1-3** and other already reported for related compounds.<sup>16, 17, 47</sup> The crystal packing of **4** does not present significant interactions (Fig. S4).

The crystal structure of compound **5** consists of a 1D-CP (Fig. 6a, S5) where two cationic  $[\text{K}(\text{THF})_4]^+$  entities connected to the hexanuclear anionic complex  $[\text{Zn}_6(\mu\text{-Cl})_2(\text{SC}_6\text{H}_4\text{Cl}_2\text{S})_4(\mu\text{-KO}:\text{KO}'\text{-SC}_6\text{H}_4\text{Cl}(\text{ClO}_2)\text{S})_2]^{2-}$  *via* both two chloride ligands and two oxygen atoms of the  $[\text{SC}_6\text{H}_4\text{Cl}(\text{ClO}_2)\text{S}]$  ligands. The cationic  $[\text{K}(\text{THF})_4]^+$  moieties show both potassium atoms linked to four oxygen atoms of the THF terminal ligands, and three bridging ligands, one oxygen atom from the  $[\text{SC}_6\text{H}_4\text{Cl}(\text{ClO}_2)\text{S}]$  unit and two chloride atoms, therefore giving rise to a highly distorted pentagonal bipyramid coordination environment (Fig. 6b).

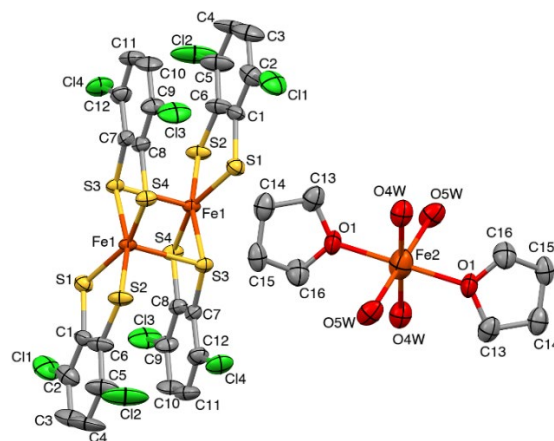
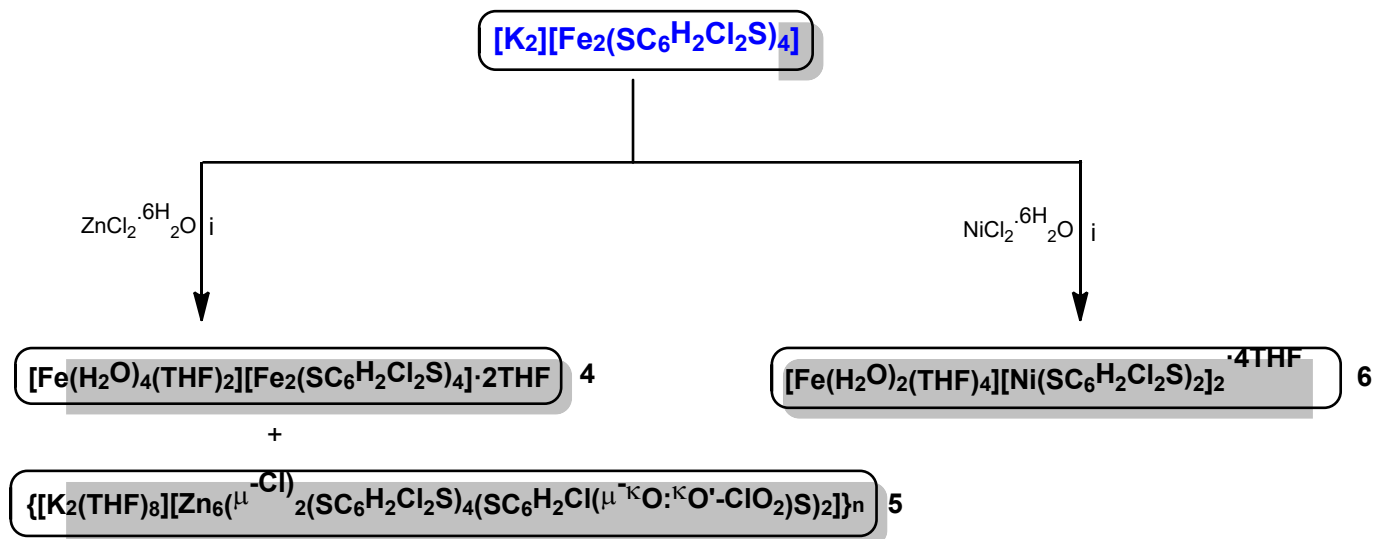


**Fig. 5.** ORTEP diagram of the molecular unit of compound **4**. Hydrogen atoms and solvent molecules have been omitted for clarity. Thermal ellipsoids are drawn at 50 % probability.

The O(1) and O(2) atoms are located in the axial positions [170.1(3)°], while the basal coordination sites are occupied by O(3), O(4), O(6) and two chlorine Cl(7) ( $\text{S} = 362.3^\circ$ ).



### i. Crystallization in THF/*n*-Heptane

**Scheme 3.** Summary of reactions to obtain compounds 4-6.

The two chlorine atoms are acting as triple bridging ligands connecting the two potassium centers and the metal entities. O(1) and O(2) atoms are located in the axial positions [170.1(3)°], while the basal coordination sites are occupied by O(3), O(4), O(6) and two chlorine Cl(7) ( $S = 362.3^\circ$ ). The two chlorine atoms are acting as triple bridging ligands connecting the two potassium centers and the metal entities.

cooling down from room temperature (Fig. 7). In compound 1, the presence of paramagnetic impurities becomes evident as  $\chi_{MT}$  product reaches a small plateau between 40-60 K. These paramagnetic impurities are probably isolated  $[Fe(dithio)_2]^-$  entities or metal vacancies on the iron dimeric entities. Finally, a further decrease is observed at temperatures below 30 K due to the presence of supramolecular interactions. Depending on the amount of these paramagnetic impurities a maximum on the susceptibility curve can be observed (compound 3) or not. Almost all Fe(III) bis-dithiolate complexes studied in detail present an intermediate spin  $S = 3/2$  configuration.<sup>16,48-50</sup> There is only one example of a low spin  $S = 1/2$  configuration.<sup>51</sup> Therefore, the data were successfully fitted to an expression that considers the presence of paramagnetic impurities, a temperature independent term, A, and a contribution of antiferromagnetically coupled  $S = 3/2$  dimers (Eq. 1).<sup>52</sup>

$$\chi_M = A + y \frac{g^2}{8T} S(S+1) + (1-y) \frac{2Ng^2\mu_B^2}{kT} \frac{e^{\frac{J}{kT} + 5e^{\frac{J}{kT}} + 14e^{\frac{J}{kT}}}}{1 + 3e^{\frac{J}{kT}} + 5e^{\frac{J}{kT}} + 7e^{\frac{J}{kT}}} \quad (1)$$

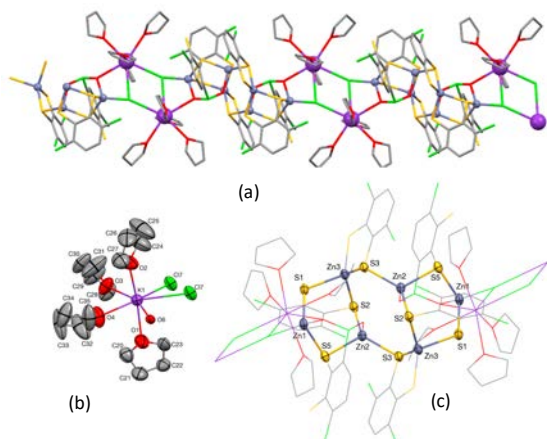


**Fig. 6.** a) Partial view of the crystal packing found for compound 5 along (44-1). (b) Simplified view of the cationic entities. (c)  $[Zn_6(\mu-Cl)_2(SC_6H_2Cl_2S)_4(\mu-\kappa O:\kappa O'-SC_6H_2Cl(ClO_2)S)_2]^{2-}$  linked to the cationic fragments showing an ORTEP drawing of the structural  $Zn_3S_3$  hexagonal and the  $Zn_4S_4$  octagonal rings. Hydrogen atoms have been omitted for clarity. Thermal ellipsoids are drawn at 50 % probability.

The magnetic behaviour of all the previous compounds is expected to be dominated by the antiferromagnetic intradimer interaction typical of all other known Fe(III) bis-dithiolate dimeric complexes containing a  $Fe_2S_2$  core.

The magnetic susceptibility data of compounds 1-3 shows a similar trend with a continuous decrease of the  $\chi_{MT}$  value upon

[Escriba aquí]



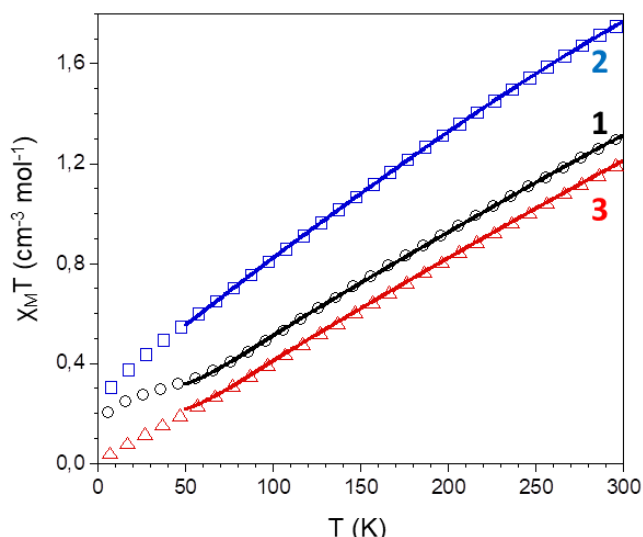


**Fig. 7.** Thermal variation of the  $\chi_M T$  product per  $[\text{Fe}_2(\text{SC}_6\text{H}_2\text{Cl}_2\text{S})_4]^{2-}$  dimer. The solid line corresponds to the best fit. Compounds: **1** (black circles), **2** (blue squares) and **3** (red triangles).

Here  $N$  is the Avogadro's number,  $g$  the Landé factor,  $\mu_B$  the Bohr magneton and  $J$  the intradimer antiferromagnetic coupling parameter (Hamiltonian). Table 2 provides the results of the fit of the experimental data. The obtained values for compounds **1** and **3** agree with the values usually reported for these kind of compounds.<sup>48–50</sup> The value calculated for compound **2** differ significantly from the others probably due to the structural distortions that the coordination of barium counterion to the sulfur atoms of the dithiolate generates, but the high amount of paramagnetic impurities present in the sample makes the obtained exchange parameter not to be very reliable. On the other hand, the small amount of compound **4** obtained in the reaction does not allow magnetic studies to be carried on it.

**Table 2.** Magnetic properties of compounds **1–3**.

compound	S	g	J (cm <sup>-1</sup> )	c (%) <sup>a</sup>
<b>1</b>	3/2	1.99	-160	7.7
<b>2</b>	3/2	1.97	-117	13.0
<b>3</b>	3/2	1.99	-161	5.2

<sup>a</sup>Paramagnetic isolated Fe(III) impurity with intermediate  $S=3/2$  spin configuration.

On the other hand, the hexanuclear zinc entity can be defined as two  $\text{Zn}_3\text{S}_3$  hexagonal chair-like ring structures connected *via* two sulfur atoms of two different  $(\text{SC}_6\text{H}_2\text{Cl}_2\text{S})$  ligands giving rise to an octagonal  $\text{Zn}_4\text{S}_4$  ring. Although connectivity between  $\text{Zn}_3\text{S}_3$  rings can be found in other reported molecules/polymers<sup>53–57</sup> most of them show an adamantane-like structure, only the complex reported by Yamada<sup>53</sup> show the same structural disposition present in compound **5** although the  $\text{Zn}_3\text{S}_3$  moieties show a boat conformation.

In compound **5** (Fig.6c), the three zinc atoms of the  $\text{Zn}_3\text{S}_3$  moieties display a tetrahedral geometry where Zn(3) fills the four coordination sites with two chelate  $(\text{SC}_6\text{H}_2\text{Cl}_2\text{S})$  ligands perpendicularly situated ( $89.1^\circ$ ), while Zn(1) and Zn(2)

environments show two and three sulfur atoms, belonging to different dithiolene units, together with Cl(7) in the case of Zn(1), and both are strongly tight by a bridging chlorite ligand from a recently formed  $[\text{SC}_6\text{H}_2\text{Cl}(\text{ClO}_2)\text{S}]$  moiety (Fig. S6). No significant interactions have been found in the crystal packing of **5** (Fig. S7).

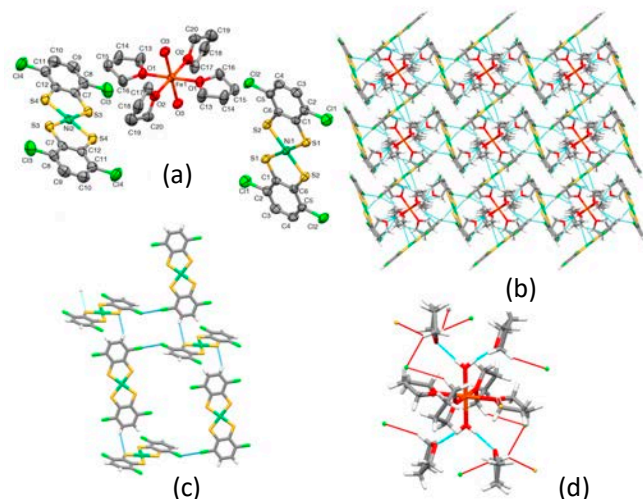


**Fig. 8.** (a) ORTEP diagram of the molecular unit of compound **6**, hydrogen atoms have been omitted for clarity. Thermal ellipsoids are drawn at 50 % probability. (b) Crystal packing found for compound **6** along (010), together with (c) C-H...S and C-Cl...Cl-C weak interactions between  $[\text{Ni}(\text{SC}_6\text{H}_2\text{Cl}_2\text{S})_2]^-$  anionic units and (d) C-H...O, C-H...Cl and C-H...S connectivity shown by the  $[\text{Fe}(\text{OH}_2)_2(\text{OC}_4\text{H}_8)_4]^{2+}$  moiety with four THF crystallization molecules and the anionic fragments.

Taking into account that the formation of two Cl-O bonds, in one of the Cl substituents in the aromatic ring of the dithiolene, is observed in compound **5**, we have considered interesting to evaluate the behavior of  $\text{ZnCl}_2 \cdot 6\text{H}_2\text{O}$  in a similar reaction with  $\text{K}_2[\text{Fe}_2(\text{SC}_6\text{H}_4\text{S})_4]$  as starting material, due to the absence of the donor chlorine substituent in this compound. But unfortunately, we were not able to obtain suitable crystals for X-ray diffraction studies, by crystallization of the residue obtained in this reaction.

Additionally, the reaction carried out with  $\text{NiCl}_2 \cdot 6\text{H}_2\text{O}$  produce a complete metathesis reaction with the formation of compound **6** (Scheme 3). This compound is made by two anionic  $[\text{Ni}(\text{SC}_6\text{H}_2\text{Cl}_2\text{S})_2]^-$  moieties instead of the dianionic  $[\text{Fe}_2(\text{SC}_6\text{H}_2\text{Cl}_2\text{S})_4]^{2-}$  found in compound **4** and a cationic  $[\text{Fe}(\text{OH}_2)_2(\text{OC}_4\text{H}_8)_4]^{2+}$  moiety. The Fe(II) monomeric entity present in compounds **4** and **6** (Fig. 5 and 8a) are similar but curiously with the opposite ratio of number of ligands THF/ $\text{H}_2\text{O}$ . Thus, the iron atom in compound **6**, the iron atom is coordinated to two oxygen atoms of  $\text{H}_2\text{O}$  molecules and four from the THF ligands, leading to six Fe-O practically identical bond distances (see range in Table 1). The TXRF analysis confirmed a Fe:Ni ratio of 1:2 and temperature variable susceptibility measurements (Fig. 9) confirm the presence of Fe(II) and Ni(III) metal centers.

The room temperature  $\chi_M T$  per formula is  $4.045 \text{ cm}^3 \text{ mol}^{-1}$  which is quite close to the expected value for 1  $\text{Fe}^{2+}$  ( $S=2$ ) and

2  $\text{Ni}^{3+}$  ( $S = 1/2$ ) isolated metal centres which would be  $3.75 \text{ cm}^3 \text{ mol}^{-1}$  (assuming  $g = 2.00$ ). The  $\chi_{\text{M}}T$  product smoothly decrease upon cooling below 150 K to achieve a  $1.156 \text{ cm}^3 \text{ mol}^{-1}$  value at 2 K. It could be due to the presence of some significant supramolecular antiferromagnetic interactions or due to zero-field splitting of the  $S=2$  spin state of  $\text{Fe(II)}$ .

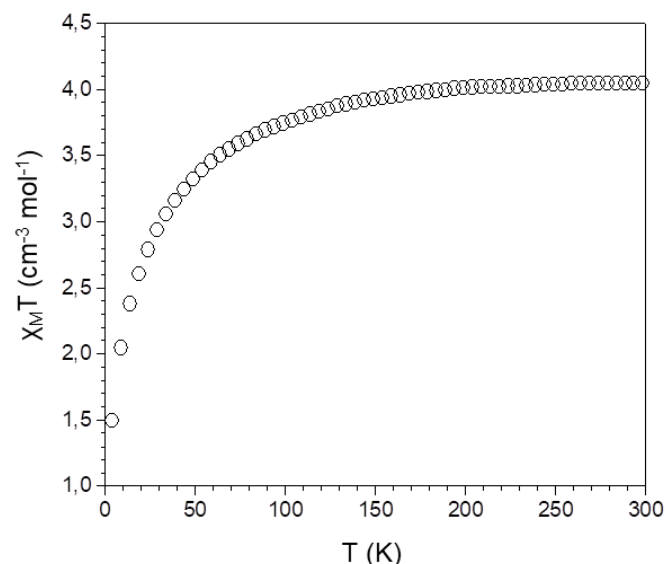


Fig. 9. Thermal variation of the  $\chi_{\text{M}}T$  product per formula in compound 6.

Respect to the crystal packing (Fig. 8), the  $\text{C}(3)\text{--H}(3)\cdots\text{S}(4)$  weak interactions between both anionic moieties in **6** are responsible for the construction of the chains (vertical chains in Fig. 8c). On the other hand, to understand the overall 3D network (Fig. 8b) is necessary to consider the existence of type-I  $\text{Cl}(1)\cdots\text{Cl}(4)$  halogen bonding interactions<sup>35, 36</sup> of  $3.366(2) \text{ \AA}$ , ( $0.14 \text{ \AA}$  shorter than the sum of the van der Waals radii) and angles of  $\text{C}(2)\text{--Cl}(1)\text{--Cl}(4)$   $145.9(1)^\circ$  and  $\text{C}(11)\text{--Cl}(4)\text{--Cl}(1)$   $149.3(2)^\circ$  (Fig. 8c), together with  $\text{C}\cdots\text{Cl}$ ,  $\text{C}\cdots\text{S}$  and  $\text{O}\cdots\text{O}$  interactions where some atoms of the  $[\text{Fe}(\text{OH})_2(\text{OC}_4\text{H}_8)_4]^{2+}$  unit are involved (Fig. 8d; additional geometrical data in ESI). Finally, we have decided to evaluate how a change in the crystallization conditions of the starting material  $\text{K}_2[\text{Fe}_2(\text{SC}_6\text{H}_4\text{S})_4]$  could afford a different CP that the one obtained previously by us using THF/*n*-Heptane at room temperature.<sup>17</sup> Thus, when the crystallization was carried out in EtOH/ $\text{H}_2\text{O}$  at  $5^\circ\text{C}$  the new 2D coordination polymer  $\{[\text{K}_2(\mu\text{-O}(\text{H})\text{CH}_2\text{Me})_2][\text{Fe}_2(\text{SC}_6\text{H}_4\text{S})_4]\}_n$  **7** (Fig. 10) was obtained instead the 1D CP  $\{[\text{K}_2(\text{OC}_4\text{H}_8)_4][\text{Fe}_2(\text{SC}_6\text{H}_4\text{S})_4]\}_n$ .<sup>17</sup>

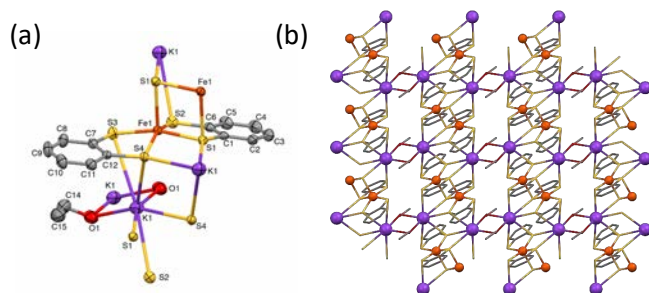


Fig. 10. ORTEP diagram of the molecular unit and crystal packing of compound **7**, view along (001). Hydrogen atoms have been omitted for clarity. Thermal ellipsoids are drawn at 50 % probability.

As depicted in Fig. 10, the  $[\text{Fe}_2(\text{SC}_6\text{H}_4\text{S})_4]^{2-}$  entities are held together through potassium cations coordinated to the sulfur atoms of the dithiolene ligands. The dinuclear iron fragments show a close resemblance to that described for compound  $\{[\text{K}_2(\mu\text{-H}_2\text{O})_2(\text{THF})_2][\text{Fe}_2(\text{SC}_6\text{H}_4\text{S})_4]\}_n$ .<sup>17</sup> The iron atoms exhibit an elongated square pyramid geometry with apical Fe–S distances [ $2.456(1) \text{ \AA}$ ] longer than those of the equatorial plane [ $2.224(1)\text{--}2.239(1) \text{ \AA}$ ]. Additionally, the potassium cations show a mono capped distorted octahedral coordination geometry (Fig. 8) that involves five sulfur atoms from the three closest  $[\text{Fe}_2(\text{SC}_6\text{H}_4\text{S})_4]^{2-}$  entities and two ethanol ligands. In this sense, S(3) and S(2) occupy the axial positions (bond angle  $\text{S}(2)\text{--K}(1)\text{--S}(3) = 172.34(3)^\circ$ ), while two O(1), S(1), and S(4) fill the equatorial sites [angles in the range  $55.09(2)\text{--}116.07(5)^\circ$ ,  $S = 357.6^\circ$ ], and a second S(4) is capping the face constituted by S(3), S(1) and other S(4).

## Experimental

All the reagents and solvents are commercially available and were used as received without further purification. Syntheses of compounds **1–7** were carried out under argon atmosphere using degassed solvents. Elemental analyses were performed on an LECO CHNS-932 Elemental Analyzer. TXRF measures were performed on a Bruker S2 PicoFox Spectrometer.

**Crystal structure determination of complexes 1–7.** Single crystals of compounds **1–7** were coated with mineral oil and mounted on Mitegen MicroMounts with the aid of a microscope and immediately placed in the low temperature nitrogen stream of the diffractometer. The intensity data sets were collected at 200 K on a Bruker-Nonius KappaCCD diffractometer equipped with an Oxford Cryostream 700 unit **1–3** or a Bruker D8 KAPPA series II with the APEX II area-detector system **4–7**, both equipped with graphite-monochromated Mo  $\text{K}\alpha$  radiation ( $\lambda = 0.71073 \text{ \AA}$ ). Most crystals of complexes **1–7** diffract weakly and data collections could only be performed up to  $q \approx 25^\circ$ , except compound **f 3** ( $27.5^\circ$ ) or the weakest **4** ( $24.1^\circ$ ). WINGX<sup>58</sup> **1–3** or Bruker SHELXTL<sup>59</sup> (**4–7** software packages were used for space group determination, structure solution, and refinement. Structures were solved by direct methods (SHELXS-97 for **1**, **2**, and **4–7**; SHELXS-2013 for **3**)<sup>60</sup> and refined by least-squares against  $F^2$  (SHELXL-2017 for **1–3**, and **4–7**; SHELXL-97 for **6**).<sup>61</sup> All the hydrogen atoms were positioned geometrically and refined by using a riding model, except those of the water molecules in compounds **1** and **6**, and H10 of the ethanol molecule in complex **7**, that were located in the Fourier difference map and refined isotropically. On the other hand, water hydrogen atoms in complex **4** could not be found in the Fourier difference map. All the non-hydrogen atoms were refined anisotropically. EADP restraints were applied to C=O groups in the acetone molecules linked to Ba1 in compound **2**. On the other hand, complex **3** crystallized with several *N,N*-



dimethylformamide disordered solvent molecules, unfortunately it was not possible to obtain a sensible chemical model and Squeeze<sup>62</sup> procedure was applied to remove their contribution to the structure factors.

Crystallographic data for compounds **1–7** are summarized in Table S1 (CCDC 1834784 (**1**), 1834781 (**2**), 1834783 (**3**), 1834785 (**4**), 1834789 (**5**), 1834786 (**6**), 1834788 (**7**)).

**Magnetic measurements of compounds 1–3 and 6.** They were performed on polycrystalline samples taken from the same uniform batch used for the structural determination with a Quantum Design SQUID susceptometer covering the temperature range 2–300 K at a magnetic field of 1 kOe.

**Synthesis of compound [Ca(H<sub>2</sub>O)<sub>3</sub>(OCMe<sub>2</sub>)<sub>4</sub>][Fe<sub>2</sub>(SC<sub>6</sub>H<sub>2</sub>Cl<sub>2</sub>S)<sub>4</sub>]**·3** OCMe<sub>2</sub> **1.** A mixture of HSC<sub>6</sub>H<sub>2</sub>Cl<sub>2</sub>SH (157 mg, 0.74 mmol) and 10 ml of an aqueous suspension of CaO (5 wt%) was stirred for 15 min. Then, a solution of FeCl<sub>3</sub>·6H<sub>2</sub>O (100 mg, 0.37 mmol) in 10 mL of EtOH/H<sub>2</sub>O (1/1) was slowly added and stirred for 30 min. The solid was filtered-off, washed with H<sub>2</sub>O and *n*-Heptane. Further crystallization from acetone/*n*-hexane (1/1) yielded to suitable crystals (90 mg, 24.6 % yield) for X-ray diffraction studies of compound [Ca(H<sub>2</sub>O)<sub>3</sub>(OCMe<sub>2</sub>)<sub>4</sub>][Fe<sub>2</sub>(SC<sub>6</sub>H<sub>2</sub>Cl<sub>2</sub>S)<sub>4</sub>]**·3** OCMe<sub>2</sub> **1**. Anal. Calcd. (Found) for C<sub>42</sub>H<sub>50</sub>CaCl<sub>8</sub>Fe<sub>2</sub>O<sub>9</sub>S<sub>8</sub> (**1**-OCMe<sub>2</sub>): C, 36.27 (36.51); H, 3.62 (3.36); S, 18.44 (17.74).**

**Synthesis of compound [Ba(OCMe<sub>2</sub>)<sub>6</sub>][Fe<sub>2</sub>(SC<sub>6</sub>H<sub>2</sub>Cl<sub>2</sub>S)<sub>4</sub>] **2.** Following the same procedure as that described for compound **1**, but using an aqueous suspension (10 mL) of Ba(OH)<sub>2</sub>·8H<sub>2</sub>O (5 wt%) instead, crystals of compound [Ba(OCMe<sub>2</sub>)<sub>6</sub>][Fe<sub>2</sub>(SC<sub>6</sub>H<sub>2</sub>Cl<sub>2</sub>S)<sub>4</sub>] **2** (130 mg, 32.4 % yield) were obtained upon crystallization of the solid residue by slow diffusion of *n*-Heptane into an acetone solution (1:1). Anal. Calcd. (Found) for C<sub>36</sub>H<sub>32</sub>BaCl<sub>8</sub>Fe<sub>2</sub>O<sub>4</sub>S<sub>8</sub> (**2**-2OCMe<sub>2</sub>): C, 32.81 (32.42); H, 2.45 (2.81); S, 19.47 (17.98).**

**Synthesis of compound [Zn(DMF)<sub>6</sub>][Fe<sub>2</sub>(SC<sub>6</sub>H<sub>2</sub>Cl<sub>2</sub>S)<sub>4</sub>] **3.** Following the same procedure as that described for compound **1**, but using an aqueous suspension (10 mL) of an aqueous suspension of Zn(OH)<sub>2</sub> (5 wt%) instead, crystals of compound [Zn(DMF)<sub>6</sub>][Fe<sub>2</sub>(SC<sub>6</sub>H<sub>2</sub>Cl<sub>2</sub>S)<sub>4</sub>] **3** (240 mg, 30.1 % yield) were obtained upon extracting the solid residue in DMF and further crystallization by slow diffusion of CH<sub>2</sub>Cl<sub>2</sub> into a DMF solution. Anal. Calcd. (Found) for C<sub>36</sub>H<sub>36</sub>Cl<sub>8</sub>Fe<sub>2</sub>N<sub>4</sub>O<sub>4</sub>S<sub>8</sub>Zn (**3**-2DMF): C, 33.11, (32.74); H, 2.78, (2.91); N, 4.29, (4.22); S, 19.64, (18.95).**

**Reaction of K<sub>2</sub>[Fe<sub>2</sub>(SC<sub>6</sub>H<sub>2</sub>Cl<sub>2</sub>S)<sub>4</sub>] with ZnCl<sub>2</sub>·6H<sub>2</sub>O.** To a THF (10 ml) solution of compound K<sub>2</sub>[Fe<sub>2</sub>(SC<sub>6</sub>H<sub>2</sub>Cl<sub>2</sub>S)<sub>4</sub>] prepared by a method previously reported by us<sup>16</sup> from 100 mg of FeCl<sub>3</sub>·6H<sub>2</sub>O, a solution of ZnCl<sub>2</sub>·6H<sub>2</sub>O (44 mg, 0.19 mmol) in 2 mL EtOH/H<sub>2</sub>O (1:1) was added. The mixture was stirred for 2 days, filtered and the solvent removed. Then, the solid residue crystallized in THF/*n*-Heptane (1:1) at 5 °C yielded few crystals of a mixture of compounds [Fe(H<sub>2</sub>O)<sub>4</sub>(THF)<sub>2</sub>][Fe<sub>2</sub>(SC<sub>6</sub>H<sub>2</sub>Cl<sub>2</sub>S)<sub>4</sub>]**·4**THF **4** and {[K<sub>2</sub>(THF)<sub>8</sub>][Zn<sub>6</sub>(μ-Cl)<sub>2</sub>(SC<sub>6</sub>H<sub>2</sub>Cl<sub>2</sub>S)<sub>4</sub>(μ-κO:κO'-SC<sub>6</sub>H<sub>2</sub>Cl(ClO<sub>2</sub>)S)<sub>2</sub>]}<sub>n</sub> **5**.

**Reaction of K<sub>2</sub>[Fe<sub>2</sub>(SC<sub>6</sub>H<sub>2</sub>Cl<sub>2</sub>S)<sub>4</sub>] with NiCl<sub>2</sub>·6H<sub>2</sub>O.** To a THF (10 ml) solution of compound K<sub>2</sub>[Fe<sub>2</sub>(SC<sub>6</sub>H<sub>2</sub>Cl<sub>2</sub>S)<sub>4</sub>] prepared by a method previously reported by us<sup>16</sup> from 100 mg of FeCl<sub>3</sub>·6H<sub>2</sub>O, a solution of NiCl<sub>2</sub>·6H<sub>2</sub>O (44 mg, 0.19 mmol) in 2 mL EtOH/H<sub>2</sub>O (1:1) was added. The mixture was stirred for 1.5

days, filtered and the solvent removed. Then, the solid residue was crystallized in THF/*n*-Heptane (1:2) yielding to suitable crystals for X-ray diffraction, confirming the formation of compound [Fe(H<sub>2</sub>O)<sub>2</sub>(THF)<sub>4</sub>][Ni(SC<sub>6</sub>H<sub>2</sub>Cl<sub>2</sub>S)<sub>2</sub>]**·4**THF **6** (70 mg, 23.8 % yield). Anal. Calcd. (Found) for C<sub>24</sub>H<sub>12</sub>Cl<sub>8</sub>FeNi<sub>2</sub>O<sub>2</sub>S<sub>8</sub> (**6**-8THF): C, 27.57 (27.24); H, 1.16, (1.16); S, 24.53 (24.03).

**Synthesis of the CP {[K<sub>2</sub>(μ-O(H)CH<sub>2</sub>Me)<sub>2</sub>][Fe<sub>2</sub>(SC<sub>6</sub>H<sub>4</sub>S)<sub>4</sub>]}<sub>n</sub> **7.** Compound K<sub>2</sub>[Fe<sub>2</sub>(SC<sub>6</sub>H<sub>4</sub>S)<sub>4</sub>] was prepared following the method previously described.<sup>17</sup> Then the residue was crystallized in EtOH/H<sub>2</sub>O (1:3) at 5 °C yielding to suitable crystals for X-ray diffraction of compound {[K<sub>2</sub>(μ-O(H)CH<sub>2</sub>Me)<sub>2</sub>][Fe<sub>2</sub>(SC<sub>6</sub>H<sub>4</sub>S)<sub>4</sub>]}<sub>n</sub> **7** (87 mg, 37.5 % yield) Anal. Calcd. (Found) for C<sub>28</sub>H<sub>28</sub>Fe<sub>2</sub>K<sub>2</sub>O<sub>2</sub>S<sub>8</sub> **7**: C, 39.90 (39.18); H, 3.35, (3.40); S, 30.43 (25.96).**

## Conclusions

In summary, the reactions carried out between HSC<sub>6</sub>H<sub>2</sub>Cl<sub>2</sub>SH, FeCl<sub>3</sub>·6H<sub>2</sub>O and divalent metal bases as deprotonating agents, lead to the isolation of ion-pair metal complexes or a neutral trinuclear compound but do not form CPs. These results suggest that under the reaction condition studied the dicationic entities ML<sub>n</sub><sup>2+</sup> (M= Ca<sup>2+</sup>, Ba<sup>2+</sup> or Zn<sup>2+</sup>) are not able to find an arrangement to bridge the dianionic [Fe<sub>2</sub>(SC<sub>6</sub>H<sub>2</sub>Cl<sub>2</sub>S)<sub>4</sub>]<sup>2-</sup> moieties as it happen in the similar reactions with alkali metals as counter cations.<sup>16, 17</sup>

Then, we have searched the possibility to prepare polymers replacing the two potassium atoms in compound K<sub>2</sub>[Fe<sub>2</sub>(SC<sub>6</sub>H<sub>4</sub>S)<sub>4</sub>] by a divalent cation such Zn<sup>2+</sup> or Ni<sup>2+</sup>. In this case the ion pair compounds [Fe(H<sub>2</sub>O)<sub>4</sub>(THF)<sub>2</sub>][Fe<sub>2</sub>(SC<sub>6</sub>H<sub>2</sub>Cl<sub>2</sub>S)<sub>4</sub>]**·4**THF and [Fe(H<sub>2</sub>O)<sub>2</sub>(THF)<sub>4</sub>][Ni(SC<sub>6</sub>H<sub>2</sub>Cl<sub>2</sub>S)<sub>2</sub>]**·4**THF together with the CP {[K<sub>2</sub>(THF)<sub>8</sub>][Zn<sub>6</sub>(μ-Cl)<sub>2</sub>(SC<sub>6</sub>H<sub>2</sub>Cl<sub>2</sub>S)<sub>4</sub>(μ-κO:κO'-SC<sub>6</sub>H<sub>2</sub>Cl(ClO<sub>2</sub>)S)<sub>2</sub>]}<sub>n</sub> were isolated. It is remarkable that although the reaction was carried out under anaerobic conditions, two Cl-O bonds were formed in the CP with Zn(II) probably due to the presence of air into the organic solvents used in this synthesis. This fact is quite surprising considering that in the d<sup>10</sup> metal dithiolene chemistry, oxidation of sulfur atoms to give sulfinate [M-S(O)<sub>2</sub>R], sulfonate [M-S(O)R] or sulfonate [M-OS(O)<sub>2</sub>R] groups is quite common but never reported before for chloro-dithiolene derivatives.

## Conflicts of interest

There are no conflicts to declare.

## Acknowledgements

This work was supported in part by MICINN (grant MAT2016-77608-C3-1-P).

## References

- 1 N. Robertson and L. Cronin, *Coord. Chem. Rev.*, 2002, **227**, 93-127.

- 2 *Dithiolene Chemistry: Synthesis, Properties and applications*, John Wiley & Sons, Inc., New York, 2004.
- 3 U. T. Muller-Westerhoff and B. Vance, *Comprehensive coordination chemistry*, Pergamon Press, Oxford, U. K., 1987.
- 4 P. I. Clemenson, *Coord. Chem. Rev.*, 1990, **106**, 171-203.
- 5 S. Ezzaher, A. Gogoll, C. Bruhn and S. Ott, *Chem. Commun.*, 2010, **46**, 5775-5777.
- 6 L. Alcácer and H. Novais, in *Extended Linear Chain Compounds.*, ed. ed. J. S. Miller, Springer US, New York, 1983, 319-351.
- 7 P. Cassoux, L. Valade, H. Kobayashi, A. Kobayashi, R. A. Clark and A. E. Underhill, *Coord. Chem. Rev.*, 1991, **110**, 115-160.
- 8 S. Sproules and K. Wieghardt, *Coord. Chem. Rev.*, 2010, **254**, 1358-1382.
- 9 B. Garreau de Bonneval, K. I. Moineau-Chane Ching, F. Alary, T. T. Bui and L. Valade, *Coord. Chem. Rev.*, 2010, **254**, 1457-1467.
- 10 S. Alvarez, R. Vicente and R. Hoffmann, *J. Am. Chem. Soc.*, 1985, **107**, 6253-6277.
- 11 S. Takaishi, M. Hosoda, T. Kajiura, H. Miyasaka, M. Yamashita, Y. Nakanishi, Y. Kitagawa, K. Yamaguchi, A. Kobayashi and H. Kitagawa, *Inorg. Chem.*, 2009, **48**, 9048-9050.
- 12 X. Ribas, J. C. Dias, J. Morgado, K. Wurst, I. C. Santos, M. Almeida, J. Vidal-Gancedo, J. Veciana and C. Rovira, *Inorg. Chem.*, 2004, **43**, 3631-3641.
- 13 R. Llusa, S. Uriel, C. Vicent, J. Clemente-Juan, E. Coronado, C. J. Gómez-García, B. Braña and E. Canadell, *J. Am. Chem. Soc.*, 2004, **126**, 12076-12083.
- 14 R. Llusa, S. Triguero, V. Polo, C. Vicent, C. J. Gómez-García, O. Jeannin and M. Fourmigué, *Inorg. Chem.*, 2008, **47**, 9400-9409.
- 15 A. L. Gushchin, R. Llusa, C. Vicent, P. A. Abramov and C. J. Gómez-García, *Eur. J. Inorg. Chem.*, 2013, 2615-2622.
- 16 S. Benmansour, E. Delgado, C. J. Gómez-García, D. Hernández, E. Hernández, A. Martín, J. Perles and F. Zamora, *Inorg. Chem.*, 2015, **54**, 2243-2252.
- 17 O. Castillo, F. Zamora, D. Hernández, E. Hernández, A. Martín, I. Martín and F. Zamora, *Cryst. Growth. Des.*, 2016, **16**, 5466-5478.
- 18 D. Bellamy, N. G. Connelly, G. R. Lewis and A. Guy Orpen, *Cryst. Eng. Commun.*, 2002, **4**, 51-58.
- 19 T. Yamaguchi, S. Masaoka and K. Sakai, *Acta Crystallogr.*, 2008, **E64**, 1557-1558.
- 20 X. Ren, P. Wu, W. Zhang, Q. Meng and X. Chen, *Trans. Met. Chem.*, 2002, **27**, 394-397.
- 21 A. J. Schultz and R. Eisenberg, *Inorg. Chem.*, 1973, **12**, 518-525.
- 22 U. Jayarathne, K. Williams, V. M. Kasyanenko, J. T. Mague, I. V. Rubtsov and J. P. Donahue, *Polyhedron*, 2012, **31**, 98-103.
- 23 A. I. S. Neves, I. Cordeiro, D. Belo and M. Almeida, *Cryst. Eng. Commun.*, 2009, **11**, 1046-1053.
- 24 A. R. Kennedy, P. C. Andrikopoulos, J. B. Arlin, D. R. Armstrong, N. Duxbury, D. V. Graham and J. B. A. Kirkhouse, *Chem. Eur. J.*, 2009, **15**, 9494-9504.
- 25 R. Yoshida, S. Ogasahara, H. Akashi and T. Shibahara, *Inorg. Chim. Acta*, 2012, **383**, 157-163.
- 26 O. Moers, A. Blaschette and P. G. Jones, *Acta Crystallogr.*, 1997, **C53**, 845-848.
- 27 W. H. Ojala, L. K. Lu, K. E. Albers, W. B. Gleason, T. I. Richardson, R. E. Lovrien and E. A. Sudbeck, *Acta Crystallogr.*, 1994, **B50**, 684-694.
- 28 C. J. Brown, M. Ehrenberg and H. R. Yadav, *Acta Crystallogr.*, 1984, **C40**, 58-60.
- 29 P. Suresh, C. Naga Babu, N. Sampath and G. Prabusankar, *Dalton Trans.*, 2015, **44**, 7338-7346.
- 30 E. t. Herdtweck, T. Kornprobst, R. Sieber, L. Straver and J. Plank, *Z. Anorg. Allg. Chem.*, 2011, **637**, 655-659.
- 31 Y. Zhao, L. L. Liang, K. Chen, N. M. Ji, X. J. Cheng, X. Xiao, Y. Q. Zhang, S. F. Xue, Q. J. Zhu, N. Dong and Z. Tao, *Dalton Trans.*, 2014, **43**, 929-932.
- 32 C. Spies, B. Finkler, N. Acar and G. Jung, *Phys. Chem. Chem. Phys.*, 2013, **15**, 19893-19905.
- 33 C. H. Lee, C. L. Wu, S. A. Hua, Y. H. Liu, S. M. Peng and S. T. Liu, *Eur. J. Inorg. Chem.*, 2015, **2015**, 1417-1423.
- 34 K. Neupert-laves and M. Dobler, *J. Cryst. Spect. Res.*, 1982, **12**, 271-286.
- 35 G. Cavallo, P. Metrangolo, R. Milani, T. Pilati, A. Priimagi, G. Resnati and G. Terraneo, *Chem. Rev.*, 2016, **116**, 2478-2601.
- 36 G. R. Desiraju and R. Parthasarathy, *J. Am. Chem. Soc.*, 1989, **111**, 8725-8726.
37. Murugavel, K. Baheti and G. Anantharaman, *Inorg. Chem.*, 2001, **40**, 6870-6878.
- 38 N. R. Halcovitch, M. J. Geier, C. M. Vogels, A. Decken and S. A. Westcott, *Cent. Eur. J. Chem.*, 2011, **9**, 386-390.
- 39 K. M. Fromm, *Angew. Chem. Int. Ed.*, 1997, **36**, 2799-2801.
- 40 S. Mishra, E. Jeanneau, G. Ledoux and S. Daniele, *Inorg. Chem.*, 2014, **53**, 11721-11731.
- 41 J. Jokiniemi, S. Peräniemi, J. Vepsäläinen and M. Ahlgrén, *Acta Crystallogr.*, 2009, **C65**, 165-167.
- 42 R. Postma, J. A. Kanter and A. J. M. Duisenberg, *Acta Crystallogr.*, 1983, **C39**, 1221-1225.
- 43 T. B. Faust, P. M. Usov, D. M. D'Alessandro and C. J. Kepert, *Chem. Commun.*, 2014, **50**, 12772-12774.
- 44 A. Y. Fu, D. Q. Wang and T. Yu, *Acta Crystallogr.*, 2004, **E60**, 1939-1940.
- 45 D. Q. Wang, A. Y. Fu and J. Y. He, *Acta Crystallogr.*, 2004, **E60**, 1915-1917.
- 46 O. Fuhr and D. Fenske, *Z. Anorg. Allg. Chem.*, 2000, **626**, 1822-1830.
- 47 P. Amo-Ochoa, E. Delgado, C. J. Gómez-García, D. Hernández, E. Hernández, A. Martín and F. Zamora, *Inorg. Chem.*, 2013, **52**, 5943-5950.
- 48 D. Simão, J.A. Ayllon, S. Rabaça, M.J. Figueira, I.C. Santos, R.T. Henriques, M. Almeida, *Cryst. Eng. Comm.* 2006, **8**, 658.
- 49 A.C. Cerdeira, D. Simão, I.C. Santos, A. Machado, L.C.J. Pereira, J.C. Waerenborgh, R.T. Henriques, M. Almeida, *Inorg. Chim. Acta* 2008, **361**, 3836-3841
- 50 K. Ray, E. Bill, T. Weyhermüller, K. Wieghardt, *J. Am. Chem. Soc.* 2005, **127**, 5641-5654.
- 51 H. Alves, D. Simão, H. Novais, I.C. Santos, C. Giménez-Saiz, V. Gama, J.C. Waerenborgh, R. T. Henriques, M. Almeida, *Polyhedron* 2003, **22**, 2481-2486.
- 52 R.L. Carlin, *Magnetochemistry*, Springer Verlag, Berlin, 1986.
- 53 Y. Yamada, Y. Miyashita, K. Fujisawa and K. Okamoto, *Bull. Chem. Soc. Jpn.*, 2001, **74**, 97-98.
- 54 I. G. Dance, A. Choy and M. L. Scudder, *J. Am. Chem. Soc.*, 1984, **106**, 6285-6295.
- 55 M. D. Nyman, M. Hampden-Smith and E. N. Duesler, *Inorg. Chem.*, 1996, **35**, 802-803.
- 56 M. Mikuriya, X. Jian, S. Ikemi, T. Kawahashi and H. Tsutsumi, *Bull. Chem. Soc. Jpn.*, 1998, **71**, 2161-2168.
- 57 A. Christensen, C. Mayer, F. Jensen, A. D. Bond and C. J. McKenzie, *Dalton Trans.*, 2006, 108-120.
- 58 L. J. Farrugia, *J. Appl. Cryst.*, 2012, **45**, 849-854.
- 59 Bruker Analytical X-ray Instruments, 2000.
- 60 G. M. Sheldrick, *Acta Crystallogr.*, 2008, **A64**, 112-122.
- 61 G. M. Sheldrick, *Acta Crystallogr.*, 2015, **C71**, 3-8.
- 62 A. L. Spek, *Acta Crystallogr.*, 2015, **C71**, 9-18.